Synthesis of Lamellar Isobutyl Silicates and Dispersion in Polypropylene Melts

Thuy T. Chastek,[1] Emily L. Que,[1] Phil Jarzombeck,[1] Christopher W. Macosko,[2] Andreas Stein[1]

[1]*Department of Chemistry, University of Minnesota, Minneapolis, Minnesota 55455*
[2]*Department of Chemical Engineering and Materials Science, University of Minnesota, Minneapolis, Minnesota 55455*

Received 29 March 2006; accepted 27 January 2007
DOI 10.1002/app.26315
Published online 23 April 2007 in Wiley InterScience (www.interscience.wiley.com).

ABSTRACT: A new synthetic clay, *i*C_4-LMS, which is a lamellar mesostructured silicate with isobutyl groups covalently attached to silicate sheets, was synthesized with the goal to increase the compatibility of the inorganic sheets with polypropylene (PP) in a melt-blending process. The lamellar morphology of *i*C_4-LMS was confirmed using X-ray diffraction and transmission electron microscopy. Based on ^{29}Si and ^{13}C{^{1}H} CP-MAS NMR spectra, isobutyl functional groups were attached to at least 10 mol % of silicate tetrahedral sites in the inorganic layers. These surface groups mimic the subunits in the PP chains. Samples of *i*C_4-LMS were mixed with several organic solvents and sonicated. The solvent most like PP, tetramethylpentadecane, had the highest viscosity, forming a gel which indicates very good dispersion of the clay. However, when *i*C_4-LMS was melt-blended with PP, it did not show significant increase in rheology. This modest effect on rheology may arise from fracture of *i*C_4-LMS layers as a result of the shear stresses during melt blending produced by the viscous PP. © 2007 Wiley Periodicals, Inc. J Appl Polym Sci 105: 1456–1465, 2007

Key words: lamellar mesostructures; synthetic clays; hybrid materials; silicates; composites

INTRODUCTION

Polypropylene (PP) is widely used in consumer and industrial applications because of its low density, cost, thermal stability, and solvent resistance. PP, however, has a relatively low mechanical modulus and high thermal expansion. A method to overcome these limitations is to combine PP with inorganic fillers to form composite materials. These composites can exhibit improved mechanical properties, including enhanced stiffness, strength, thermal stability, and reduced thermal expansion and flammability.[1–3] Typically 20% of micron size fillers is required to achieve these improvements. Even greater property enhancements at lower loadings can be achieved for more polar polymers, such as nylon-6, when montmorillonite-derived organoclays are dispersed throughout the polymer to form a nanocomposite with highly exfoliated clay sheets.[1,3–11] However, in the case of PP and organoclays, the improvements have been much more modest, because of poor exfoliation of clay sheets in this nonpolar polymer. To improve dispersion of clay in PP, natural clays have been modified by intercalation of surfactants or the polymer has been modified with a compatibilizer (polymers modified to include polar functional groups).[1–6,8–10,12–15]

This article describes the investigation of an alternate approach towards compatibilization of clay sheets with nonpolar polymers, namely the preparation and use of synthetic clays in which appropriate organic functional groups are covalently attached to silicate layers. The synthetic clays are prepared by sol-gel methods combined with surfactant templating, and used as synthesized. This method eliminates the cation exchange process, avoids natural impurities, and provides some flexibility in terms of organic functional groups that are decorating a silica sheet surface.

We recently reported a strategy for preparing synthetic clays with covalently attached alkyl chains (C_{16}-LMS, C_{16}-LMAS, C_{16}-SiO_2-LMAS).[16,17] Surface modification of silicate or aluminosilicate sheets with alkyl groups provided a way of modifying interactions of the clay sheets with polystyrene (PS), and incorporation of these clays in PS enhanced the elastic modulus compared to the pure polymer. However, based on rheology, the dispersion of these alkyl-modified clays in polypropylene (PP) was not good.

Here, we describe the preparation, structure, and use of a new organically-functionalized clay, *i*C_4-LMS, as a potential candidate for melt dispersion in PP. *i*C_4-LMS is a lamellar mesostructured silicate with isobutyl groups covalently attached to the inorganic sheets.

Correspondence to: A. Stein (stein@chem.umn.edu) or C. W. Macosko (macosko@umn.edu).

Contract grant sponsor: General Motors (GM).
Contract grant sponsor: Industrial Partnership for Research in Interfacial and Materials Engineering (IPRIME), University of Minnesota.
Contract grant sponsor: NSF; contract grant number: DMR-0212302.

Isobutyl groups are intended to increase the compatibility with PP because they resemble the PP backbone and they reduce the polarity of the silicate sheets. The work was motivated by the hypothesis that increased compatibility would improve dispersion and exfoliation in iC$_4$-LMS/PP composites. The iC$_4$-LMS/PP melt-blends are evaluated by comparison with blends of PP and the commercial organoclay, Cloisite® 20A, or with the synthetic mesolamellar silicate, MCM-50. Cloisite® 20A is derived from a natural montmorillonite and has 1 nm thick aluminosilicate sheets, separated by cationic dimethyl, ditallow surfactant molecules (65% C_{18}, 30% C_{16}, and 5% C_{14} surfactants), which are introduced in a separate ion-exchange step.[18] The alkyl surfactants have been found to improve the ability of clays to be dispersed in certain polymers.[2,19–27] MCM-50, a lamellar mesostructured silicate first synthesized by the Mobil Corp., incorporates a cationic surfactant, hexadecyltrimethyl ammonium bromide (CTAB, C_{16}^{+} surfactant) between the silicate layers.[28,29] Cetyltrimethylammonium bromide (CTAB) was also used as a surfactant in the synthesis of iC$_4$-LMS. In addition to the alkylammonium surfactant, iC$_4$-LMS contains isobutyl groups covalently attached to silicate sheets. Unlike the commercial clay Cloisite® 20A, the synthetic clays MCM-50 and iC$_4$-LMS do not contain metal cations in the silicate layers. Syntheses for a number of mesostructures with different organic interlayer functional groups have been reported in several other studies, a few of which also investigated the corresponding polymer-clay nanocomposites.[14,30–40]

EXPERIMENTAL

Materials

Cetyltrimethylammonium bromide (CTAB), tetraethyl orthosilicate (TEOS), and hydrochloric acid (HCl, 37 wt %) were obtained from Aldrich (Milwaukee, WI); sodium hydroxide (NaOH) from Fisher Scientific (Pittsburg, PA); isobutyltriethyl orthosilicate (iC$_4$-TEOS) from Gelest (Morrisville, PA); ethanol (200 proof) from AAPER Alcohol and Chemical (Shelbyville, KY); Cloisite® 20A (a modified natural montmorillonite with 95 mequiv/100 g clay of quaternary ammonium salt) from Southern Clay Products (Gonzales, KY); Irganox 1010 (an antioxidant) from Ciba (Tarrytown, NY); Basell (Lansing, MI) polypropylene (Profax PH020) with a melt flow index of 35 (PP-43K) and Fusabond® MD-353D, which is a Dupont (Wilmington, DE) product having a melt flow of 450, 1.40 wt % of grafted maleic anhydride, and T_m of 136°C were donated by General Motors Corp. (Warren, MI). Isotactic polypropylene, PP-7K, with a nominal molecular weight of $M_n = 5$ kg/mol and $M_w = 12$ kg/mol was purchased from Aldrich. ^{1}H and ^{13}C-NMR spectra of PP-7K dissolved in toluene-d_8 at 100°C confirmed the composition and isotactic nature of this sample. Differential scanning calorimetry showed two melting events at 148 and 158°C. The molecular weight distribution of the PP-7K sample dissolved in 1,2,4-trichlorobenzene was determined by high temperature gel permeation chromatography to be $M_n = 2.1$ kg/mol and $M_w = 6.8$ kg/mol, PDI = 3.22, using Mark–Houwink parameters for PP for calibration.[41] For PP-43K, we determined $M_n = 6$ kg/mol, $M_w = 43$ kg/mol, PDI = 7.03. All chemicals were used as received.

MCM-50 synthesis

CTAB was added to an aqueous solution of NaOH and stirred at room temperature until a homogenous solution was formed (~5 min). Then TEOS was added to the surfactant/base solution at room temperature (RT) and stirred for 30–45 min. The mixture was loaded into a Teflon-lined autoclave and heated without agitation in an oven at 150°C for 2 days. The precipitated product was collected by filtration on a Büchner funnel, washed repeatedly with distilled water, and dried under ambient conditions. Typical mole ratios of reagents for a lamellar product were: 1.00 CTAB : 2.23 TEOS : 150. H_2O : 0.818 NaOH.

iC$_4$-LMS synthesis

Using reactant mole ratios for the preparation of MCM-50 as a starting point, iC$_4$-TEOS was added to the reaction mixture at concentrations from 5 to 100% mol relative to the moles of unfunctionalized TEOS. In general, CTAB was added to an aqueous solution of NaOH and stirred for ~5 min. iC$_4$-TEOS was added to the solution and stirred for at least 45 min because of its slower rate of hydrolysis relative to TEOS. TEOS was then added to the reaction solution and stirred for 20–30 min. The pH was adjusted to 11.5 using concentrated HCl. The temperature of the reaction solution was set to a value in the range from RT to 150°C. If a temperature of 100°C or higher was required, the mixture was loaded into a Teflon-lined autoclave and heated without agitation in an oven. The reaction time ranged from 1 to 7 days. White solid products were collected by vacuum filtration on a Büchner funnel and rinsed repeatedly with distilled water. The products were dried under ambient conditions for at least 24 h. The mole ratios and reaction conditions for the optimized lamellar phase were: 1.00 CTAB : 2.00 TEOS : 0.220 iC$_4$-TEOS : 150 H_2O : 0.812 NaOH, heated for 3 days at 150°C.

Acid extraction

Surfactant extraction was performed by stirring a suspension of iC$_4$-LMS in an HCl/ethanol solution (50 mL 1.0M HCl/ethanol per 0.165 g of sample), and

refluxing at 70°C for at least 24 h. The extracted product was then filtered, washed with water, and dried in air at ambient temperature.

Dispersion of synthetic clays in solvents

The synthetic clays were dispersed into solvents with differing solubility parameters. Each solvent was mixed with 5 wt % clay and sonicated in a Branson 3510 Ultrasonicator (100 W, 42 kHz) for 1 h in a sealed 8 mL glass vial. After at least 10 days aging the vials were inverted and if no flow was observed the sample was considered to be a gel.

Polymer–clay nanocomposite preparation

The synthetic clays were blended with PP in a heated DACA twin-screw microcompounder with a typical sample size of 4 g.[42] A mixture of polymer, synthetic clay, and the antioxidant Irganox (~0.01 wt %) was compounded under nitrogen at 100 rpm for 15 min at 160°C, or 180°C. Cloisite® 20A was also blended with a compatibilizer, Fusabond®, and PP-7K, and this mixture was used to compare with PP-7K/synthetic clay mixtures prepared without Fusabond®. The samples were molded directly into 25 mm diameter, 1 mm thick disks on the rheometer plates.

Product characterization

Thermogravimetric analyses (TGA) and differential thermogravimetric analysis (DTA) were performed in a nitrogen atmosphere using a Netzsch STA 409 PC thermal analyzer. The samples were heated from 25 to 1000°C at a heating rate of 15°C/min. Powder X-ray diffraction (XRD) patterns were recorded using a Siemens D-5005 wide-angle XRD spectrometer with Cu Kα radiation, operating at 40 kV and 45 mA. Combined small and wide angle X-ray scattering (SWAXS) analysis was performed using an Anton Paar SAXSess instrument. Samples were ground into a powder using a cryogenic impact grinder (Spex 6700 Freezer/Mill) for 5 min. Approximately 10 mm^3 of the resulting powder was sealed between layers of Kapton polyimide tape (Dupont). All samples were exposed to X-rays for 10 min. The data were normalized with the beam using SAXSquant software (Anton Paar KG).

Transmission electron microscopy (TEM) images were recorded digitally using a Jeol 1210 microscope operating at 120 keV. Samples of synthetic clays were prepared by sonicating materials in absolute ethanol or toluene for 5 min, and depositing 2–3 drops of the suspension on a holey carbon grid. The samples were allowed to dry at least 30 min before imaging. Thin sections (~70 nm) of the PP nanocomposite materials were prepared by cryo-microtoming from RT to −90°C using a Reichert Jung ultra-microtome with a diamond knife. Scanning electron microscopy (SEM) was performed on the air-dried powder samples using a Jeol 6500 microscope. Samples were dusted on an adhesive conductive carbon disc attached to an aluminum mount. All samples were then coated with 9 nm of Pt.

^{29}Si MAS NMR spectra were measured using a Bruker ASX-400 spectrometer which includes a 9.4 T magnet (^{29}Si: 79.49 MHz). The ^{29}Si spectra were measured using a single pulse experiment (90° pulse width: 5.5 or 6.0 μs, spinning rate: 5.0 kHz, recycle delay: 150 s) and calibrated using tetrakistrimethylsilane (set to −9.83 ppm relative to tetramethylsilane) as a secondary standard. ^{13}C-NMR spectra were measured using a Bruker Avance DSX-400 spectrometer, employing a single pulse experiment (^{13}C: 100.61 MHz, spinning rate: 8.5 kHz, recycle delay: 5 s, pulse width: 4.0 μs, and 1000 scans). Adamantane was used as a chemical shift standard for ^{13}C (set to 38.4 ppm).

Melt state rheology data were obtained on an ARES rheometer at 180°C. Samples were measured using 25 mm diameter parallel plates with a gap of ~1 mm. Dynamic strain sweep and dynamic frequency sweep tests were performed on the melt samples. A strain sweep was performed on each sample at a frequency of 1.0 rad/s and strains from 0.1 to 100%, to determine the linear viscoelastic (LVE) region. The critical strain was determined as the strain where G' had decreased to 80% of its maximum value. The frequency sweeps were performed from 100 to 0.01 rad/s at strains within the LVE region 10 min after the strain sweep.

RESULTS AND DISCUSSION

Influence of synthesis conditions on structure of iC$_4$-LMS

The observed morphology of silicate mesostructures is known to be affected by synthesis conditions, such as reagent ratio, temperature, pH, and reaction time.[35,43–49] In this current work, the reaction time, temperature, and molar ratio of iC$_4$-TEOS to TEOS were varied to determine the optimum conditions for formation of iC$_4$-LMS with lamellar morphology. The synthesis for the known mesolamellar silicate, MCM-50, with 100% TEOS as the silicate source, was used as a starting point: 1.0 CTAB : 2.23 TEOS : 150 H_2O : 0.818 NaOH heated at 150°C for 2 days produced the most ordered lamellar phase, based on intensities and sharpness of XRD reflections. The XRD pattern of the optimized MCM-50 sample [Fig. 1(A)] showed three low-angle reflections (at 3.2, 1.6, and 1.1 nm), which is consistent with a lamellar morphology with a layer spacing of 3.2 nm.

To determine optimal conditions for producing a lamellar iC$_4$-LMS phase, a fraction of TEOS was substituted with iC$_4$-TEOS. At 150°C and a reaction time of 2 days, a lamellar phase was observed with 5–10 mol

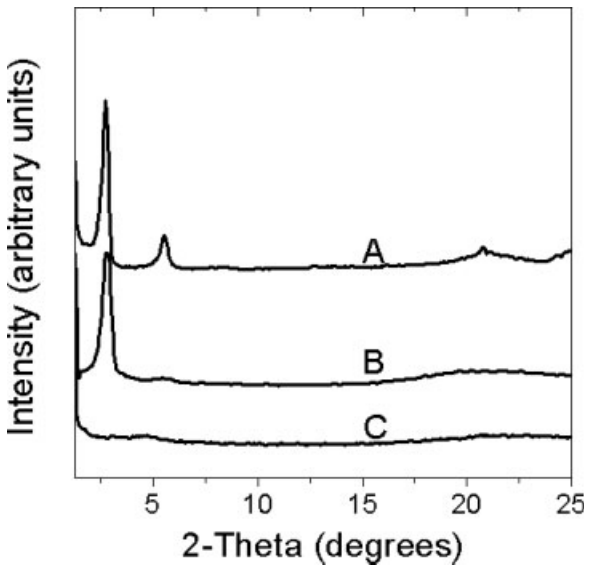

Figure 1 XRD patterns of synthetic clays (A) MCM-50, (B) iC$_4$-LMS, (C) iC$_4$-LMS-ex (after extraction of CTAB). The iC$_4$-sample was prepared at 150°C with a reaction time of 3 days and an iC$_4$-TEOS fraction of 10 mol % of total Si.

% iC$_4$-TEOS. However, with 5 mol % iC$_4$-TEOS, the product was not phase-pure and three XRD reflections were observed at low angle, corresponding to d-spacings of 3.9, 3.1, and 1.6 nm. When 10 mol % iC$_4$-TEOS was used, the XRD pattern showed only two reflections peaks (at 3.3 and 1.7 nm) corresponding to a lamellar morphology with a d_{001} reflection at 3.3 nm. Above 20 mol % of iC$_4$-TEOS, a poorly ordered mesostructure (low intensity with one XRD reflection peak) was observed. No ordered mesostructure was observed above 40 mol % iC$_4$-TEOS (no XRD reflection peak). These results indicate that isobutyl groups influence the ordering of the surfactant-templated mesostructures. Such an effect is often observed for hybrid organosilicate mesostructures prepared by cocondensation reactions.[50] With 10 mol % iC$_4$-TEOS and reagent ratios of 1.00 CTAB : 2.00 TEOS : 0.220 iC$_4$-TEOS : 150. H_2O : 0.812 NaOH, the effect of varying the reaction time from 1 day to 7 days was studied at 150°C. A lamellar morphology with the highest intensity of XRD reflections was observed for a product reacted for 3 days, with d_{001} and d_{002} spacings of 3.3 and 1.7 nm, respectively, [Fig. 1(B)]. The d-spacing value of 3.3 nm for the first order reflection peak was only slightly larger than the length of one hexadecyl group and the thickness of the silicate layer. This implies that the surfactant molecules formed an interdigitated array between isobutyl-silicate layers. A weak broad XRD reflection, which was observed at 0.42 nm, is indicative of some disorder within the inorganic layers or due a small amount of an amorphous component.[51,52] With a shorter reaction time of 1 day, a disordered mesophase (high intensity with one XRD reflection peak) was observed. After reaction times longer than 3 days, the lamellar morphology was gradually lost and became completely disordered (no d_{001} peak) after 7 days. This progression in mesostructure can be understood by considering changes in interfacial charges at the surfactant/silicate boundaries as the silicate precursors condense.[49] The lamellar phase is formed at a particular ratio of positive charges from the cationic surfactant to negative charges from the organosilicate layers. It is only kinetically stable and transforms to the disordered structure with longer hydrothermal reaction times.[53]

Acid extraction was used to remove CTAB from iC$_4$-LMS and the extracted product was denoted as iC$_4$-LMS-ex. Without the presence of CTAB, the layers collapsed, as indicated by the XRD pattern. The XRD pattern of iC$_4$-LMS-ex [Fig. 1(C)] showed only one broad first order reflection peak with low intensity at a 2θ value of 4.72°, corresponding to 1.86 nm. This is little larger than the spacing expected for adjacent iC$_4$-silicate layers and could indicate that the surfactant was mostly but not completely removed, a hypothesis that was supported by ^{13}C CP-MAS NMR (see below). However, the observed collapse supports the assignment of iC$_4$-silicate to a lamellar phase, as a condensed hexagonal or cubic phase would have remained hexagonal or cubic after surfactant extraction.

SEM images of iC$_4$-LMS showed agglomerates of irregular-shaped particles with relatively smooth and often rounded surfaces (Fig. 2). The particles had typical dimensions of several micrometers. Similar morphologies were observed for the nonfunctionalized MCM-50 samples. These particles were themselves composed of stacks of organosilicates. A TEM image of iC$_4$-LMS after sonication in ethanol [Fig. 3(A)] shows a top view of a typical thin sheet in the plane of the image with edge-to-edge dimensions of a few hundred nanometers. This sheet is composed of multiple silicate layers, evidenced by gradients in contrast

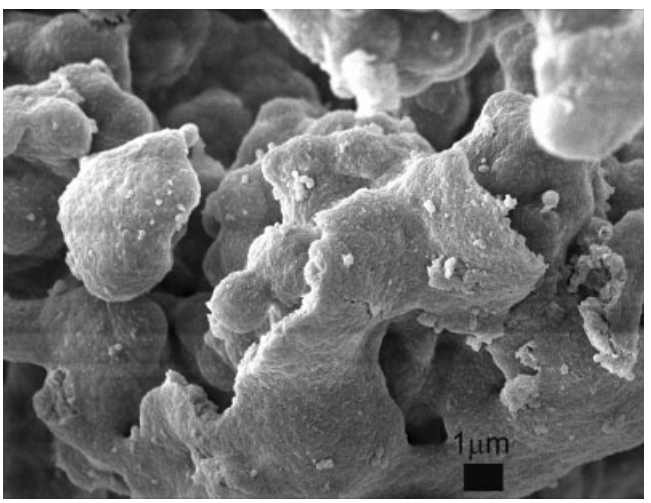

Figure 2 SEM micrograph of iC$_4$-LMS.

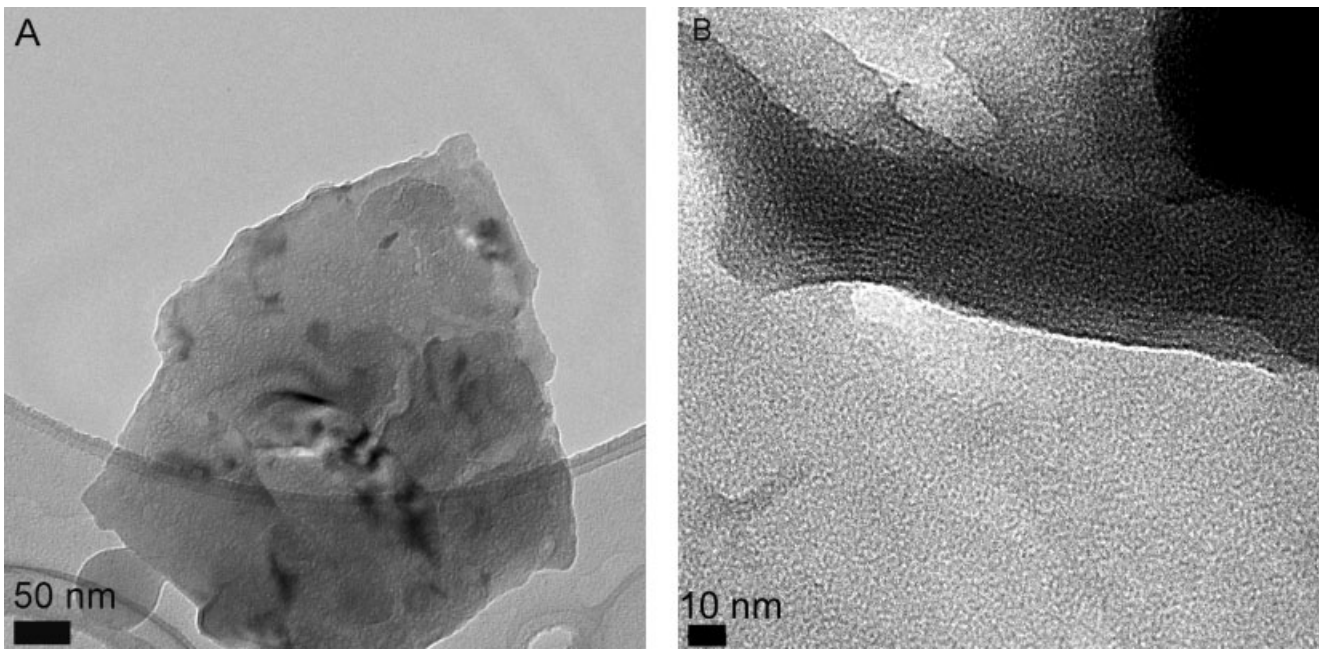

Figure 3 TEM micrographs of (A) a top view of an iC_4-LMS sheet prepared in ethanol, and (B) a side view of iC_4-LMS prepared in toluene, dried overnight, showing alternating layers of organosilica and surfactant.

throughout the particle. A side-view of another particle (which had been isolated from a sonicated iC_4-LMS dispersion in toluene) shows darker and lighter parallel lines arising from alternating silicate and surfactant layers in the mesostructure [Fig. 3(B)].

Structure of the synthetic clay layers

^{29}Si MAS NMR spectra (Fig. 4) provided information about the silicon environment in the organically functionalized clays and confirmed preservation of the Si-C bonds in the products. One can expect peaks of the type T^m, corresponding to organosiloxane groups $RSi(OSi)_m(OH)_{3-m}$ ($m = 0$–3, $R = C_4H_9$), and Q^n peaks associated with siloxane groups, $Q^n = Si(OSi)_n(OH)_{4-n}$ ($n = 0$–4). In the spectrum of the as-prepared iC_4-LMS sample [Fig. 4(A)], resonances from the T^m groups were relatively weak and the predominant peaks corresponded to Q^4 (δ, 112 ppm) and Q^3 (δ, 100 ppm) with nearly equal intensities, indicating that the silicate layers were well condensed. To enhance the

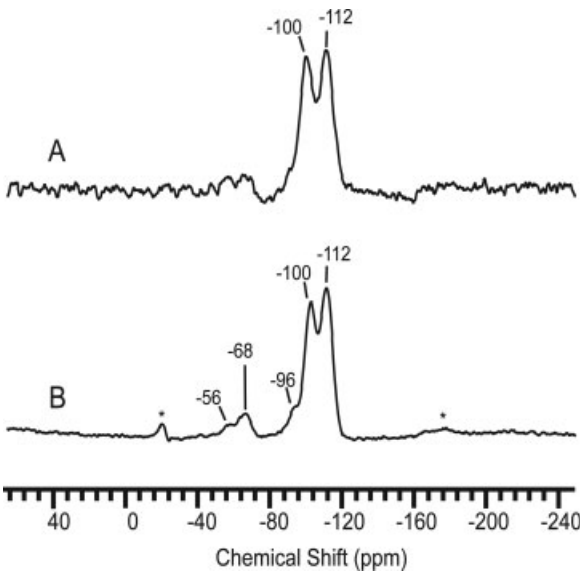

Figure 4 ^{29}Si MAS NMR spectra of iC_4-LMS: (A) as-synthesized; (B) after extraction of CTAB surfactant, iC_4-LMS-ex. The peaks marked (*) are spinning side bands.

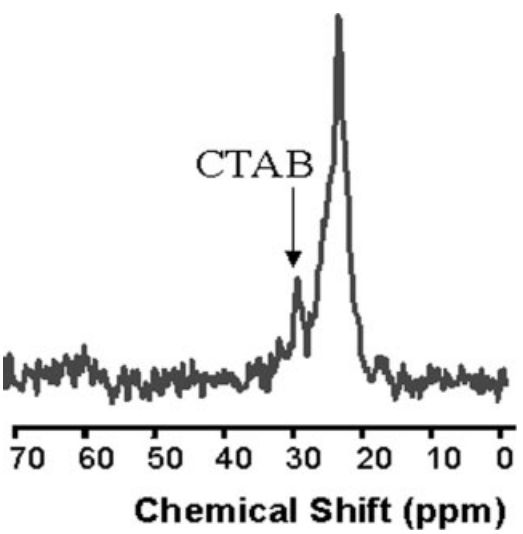

Figure 5 ^{13}C MAS NMR spectrum of iC_4-LMS-ex showing resonances due to isobutyl groups and a small amount of remaining surfactant CTAB.

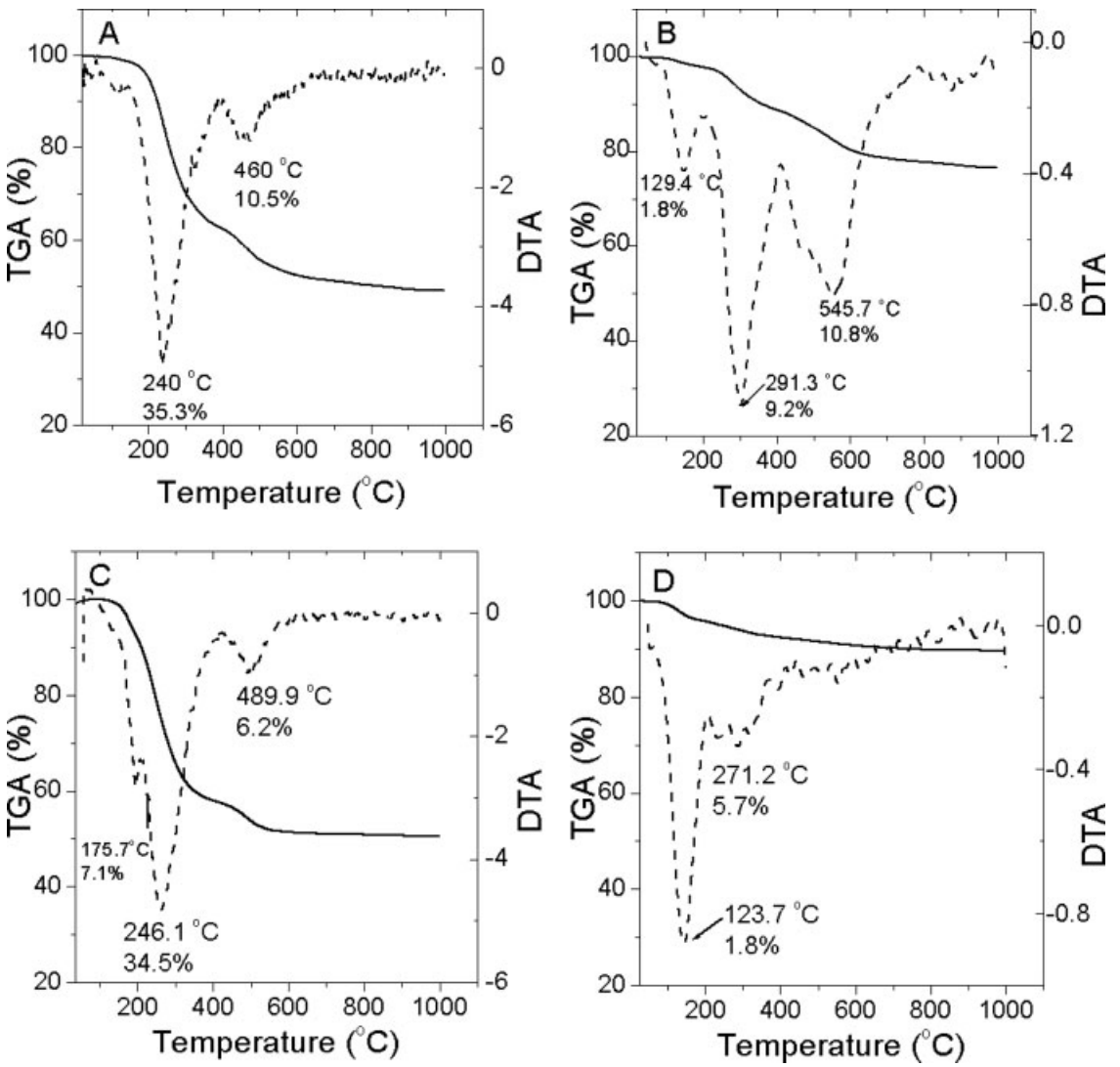

Figure 6 TGA/DTA curves for (A) *i*C_4-LMS, (B) *i*C_4-LMS-ex, (C) MCM-50, and (D) MCM-50-ex. Solid lines correspond to TGA curves (left axes) and broken lines to DTA curves (right axes).

intensity of T^m peaks, the surfactant, CTAB, was removed from *i*C_4-LMS by extraction. The ^{29}Si MAS NMR spectrum of the extracted product, denoted as *i*C_4-LMS-ex, is shown in Figure 4(B). Because the fraction of silicon in the overall sample was increased by surfactant extraction, T^3 (δ, −65 to −68 ppm; 5%) and T^2 resonances (δ, −56.2 to −59.7 ppm; 5%) could now be clearly resolved. These peaks indicated that 10% of the silicon atoms in the sample contained isobutyl groups, which were covalently attached to the silicate layers. The incorporation of *i*C_4-TEOS in the structure was therefore approximately quantitative. A Q^2 shoulder (δ, −91.6 to 96.0 ppm; 4%) was also observed in addition to the most intense Q^4 (δ, 112 ppm, 46%) and Q^3 (δ, 100 ppm, 38%) resonances.

A ^{13}C{^{1}H} CP-MAS NMR spectrum of *i*C_4-LMS-ex (Fig. 5) showed characteristic peaks of isobutyl groups, as well as those due to some remaining surfactant, CTAB. By curve-resolution of the most intense peak, resonances from isobutyl groups were identified at approximately 25.8 ppm (isobutyl end carbons ($\mathbf{C}H_3)_2$—CH—CH_2—Si), 24.1, and 23.0 ppm.[54] In addition, a small amount of surfactant CTAB was present indicated by a weak, broad —N— ($\mathbf{C}H_3)_3$ resonance near δ 63 ppm, ($\mathbf{C}H_2)_n$- resonances at δ 32.5 ppm, δ 30.0 ppm and possibly additional resonances overlapping with the isobutyl resonances.

Thermal stability of the synthetic clays is important for melt processing at elevated temperatures. The thermal behavior was investigated using TGA and DTA. To determine effects of the isobutyl groups, *i*C_4-LMS and *i*C_4-LMS-ex were compared with MCM-50 and an acid-extracted form, MCM-50-ex, from which CTAB had been removed. The TGA curves of all four clays (Fig. 6) showed a small weight loss between ca. 105 and 175°C, which was due to loss of surface-adsorbed water. In the nonextracted clays, the decomposition of surfactant alkyl chains occurred between

TABLE I
Effect of Solvent Type on Viscosity of 5 wt % Clay Dispersion

Solvent or polymer	Solubility parameter ($MPa^{1/2}$)[a]	Observations[b] MCM-50	iC_4-LMS
Hexane	14.9	+	+
2,6,10,14-TMPD	15.0[c]	+	Gel
Xylene	18.0	Gel	+
Toluene	18.2	Gel	+
THF	18.6	+	+
Styrene	19.0	+	+
1-Butanol	23.3	0	0

[a] Ref. 59.
[b] Visual observation: gel, no flow when inverted; +, increased viscosity but some flow when inverted; 0, no increase in viscosity.
[c] Calculated based on the method by Hoftyzer and Van Krevelen.[58]

~140 and 400°C, in a process which typically begins with Hofmann degradation to produce trimethylamine and a long-chain alkene. In the extracted clays, this event was much less pronounced but still present, indicating that surfactant extraction had not been complete. A smaller weight loss step occurred mainly between 400 and 550°C and continued at higher temperatures. This was related to condensation of silanol groups with concomitant loss of water. For MCM-50 materials, the fraction of material lost in this range was consistent with the content of silanol groups determined by ^{29}Si MAS NMR. Mass losses and DTA peaks which were unique to the iC_4-LMS and iC_4-LMS-ex samples appeared between 500–800°C and 800–1000°C in a nitrogen atmosphere. They are likely to be associated with the escape of decomposition products from isobutyl groups. Mass loss during these events was consistent with 10% of Si-groups being attached to isobutyl groups. In addition to supporting the structural model for iC_4-LMS, the thermal analysis data indicated that iC_4-LMS is stable at typical melt processing temperatures for PP.

Effect of clay on solvent viscosity

The ability of iC_4-LMS and MCM-50 to increase the viscosity of a series of solvents was investigated. This rapid screening test provides an initial indication of interactions between the clays and specific polymers with solubility parameters similar to those of the solvents.

Increases in the viscosity of synthetic clay-solvent mixtures were monitored visually. Even low concentrations of high aspect ratio, plate-like clay particles can lead to flocculation, caused by edge-to-face and edge-to-edge association (''house-of-cards'' structures) and result in the formation of a continuous network or gel structure.[17,55–59] Dispersions of both MCM-50 and iC_4-LMS showed viscosity increases in all the solvents listed in Table I except for 1-butanol. For MCM-50, gel formation was observed in the aromatics: toluene and xylene, while for iC_4-LMS the aliphatic 2,6,10,14-tetramethylpentadecane (TMPD), formed a gel. None of our other synthetic clays formed strong gels in TMPD.[17] Because TMPD has a structure similar to the PP backbone we were encouraged to melt blend iC_4-LMS into PP.

Dispersion of synthetic clays in PP

Nanocomposites of low molecular weight PP (PP-7K) with clay loadings of 5 wt % (corresponding to 2.5 wt % inorganic oxide content, based on TGA data) were prepared by melt blending at 180°C. Melt rheology was performed at the same temperature. There was very little increase in the elastic modulus of melts of any of the nanocomposites: iC_4-LMS, MCM-50 and Cloisite 20A with PP-7K and also with the higher molecular weight PP-43K.

SWAXS patterns of PP-7K blends with synthetic clay loadings of 2.5 wt % inorganic oxide content were obtained to determine the extent of intercalation or exfoliation of the clays. All data were normalized to the intensity of the beam to quantify the intensity. The SWAXS pattern of the pure clay, iC_4-LMS, showed two relatively broad reflection peaks at small angles corresponding to d_{001} and d_{002} values of 3.30 and 1.65 nm, respectively, [Fig. 7(A)]. This is in agreement with the XRD pattern [Fig. 1(B)] for this lamellar mesostruc-

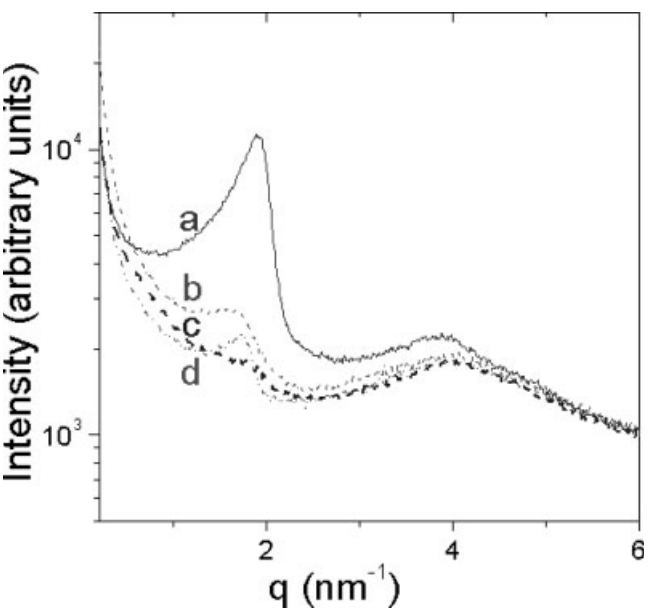

Figure 7 SWAXS patterns of (a) synthetic clay iC_4-LMS (solid line), and of the following blends: (b) PP-7K/Cloisite® 20A (dash-single-dotted line), (c) PP-7K/MCM-50 (dashed line), or (d) PP-7K/iC_4-LMS (dash-double-dotted line). The blends contained 2.5 wt % inorganic material.

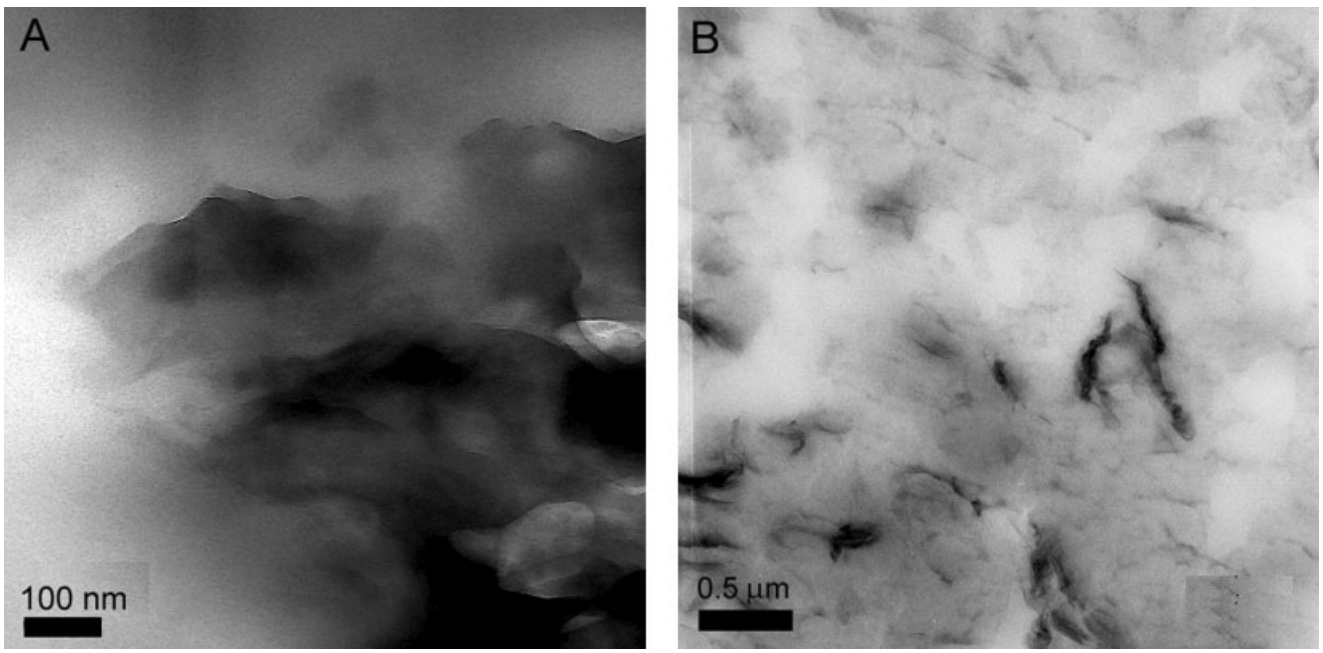

Figure 8 TEM micrographs of (A) PP-7K/iC$_4$-LMS and (B) PP-7K/Cloisite® 20A/Fusabond® blends.

ture with an approximate layer spacing of 3.3 nm. The d_{001} peak for the PP-7K/Cloisite® 20A blend shifted to 3.8 nm from a value of 2.4 nm in pure Cloisite® 20A [Fig. 7(B)]. This indicates that Cloisite® 20A particles were intercalated by a significant fraction of polymer. For MCM-50, the peak positions shifted only slightly after blending with PP, corresponding to changes in layer spacing from 3.2 nm in the pure clay to 3.6 nm in the blend [Fig. 7(C)]. This result indicates that relatively little intercalation of MCM-50 particles with PP had occurred. For blends of iC$_4$-LMS with PP, the observations were similar and layer spacings changed from 3.3 nm to 3.5 nm [Fig. 7(D)]. The reduction in d_{001} peak intensity was in part due to clay exfoliation, in part due to dilution of the clay in the composite. Partial disorder could also have reduced the X-ray intensity. The presence of this peak in the composite implied that a significant number of clay particles still contained multiple layers. It should be noted that PP-7K also displays a broad peak around $q = 4$ nm^{-1}, which overlaps with the d_{002} reflection of the clay. As a result, the intensity in this range did not vary significantly upon composite formation. Additional peaks were observed in the range from 8.0 to 18.0 nm^{-1} (not shown), corresponding to crystalline PP.

A TEM image of the PP-7K/iC$_4$-LMS blend is shown in Figure 8(A). In this and most other micrographs obtained, we could not image the edges of the iC$_4$-LMS platelets. This may be due to the lack of crystallinity within individual iC$_4$-LMS sheets and thus reduced contrast between clay sheets and PP. The shadowy features may also be related to thickness variations in the microtomed samples. Therefore, quantification of the degree of exfoliation and aspect ratios was not possible via TEM.[7,60] However, estimation of lateral sheet dimensions was possible. Before blending, a typical edge-to-edge length of iC$_4$-LMS was ~0.4 μm (Fig. 3). The edge lengths of iC$_4$-LMS particles did not decrease significantly during melt-blending, remaining between 0.2 and 1.5 μm (average: 0.48 μm for 7 particles). In agreement with the SWAXS data, stacks of sheets were still present, judging from the gradients in contrast throughout the image. Frequently, iC$_4$-LMS particles were partly curled. The flexibility may be due to the fact that organosilicate sheets in this material are not crystalline, unlike those of Cloisite® 20A. The flat shape and high crystallinity of the Cloisite® 20A sheets made it easier to observe the edges of Cloisite® 20A particles by TEM. The TEM image of a PP-7K/Cloisite® 20A/Fusabond® blend [Fig. 8(B)] showed that most of the particles were not exfoliated. Moreover, the particles were smaller than iC$_4$-LMS particles after melt blending, ranging from 0.19 to 0.23 μm (average: 0.22 μm for 7 particles).

CONCLUSIONS

The formation of PP-clay nanocomposites has been difficult up to this point, and has typically required the use of a polymeric compatibilizer that helps match polarities of clay sheets and polymer chains. In polymer-clay nanocomposite applications, attachment of functional groups to clay sheets is significant because it can modify polymer-clay interactions, which can potentially lead to better mechanical properties of the

polymer. In this work, we were able to demonstrate gel formation (one indicator of clay dispersion) in a PP-like solvent TMPD (2,6,10,14-tetramethylpentadecane) in one of our synthetic clays. The synthetic clay, iC$_4$-LMS was synthesized by templating with the cationic surfactant, CTAB and monomeric precursors, TEOS and isobutyl-substituted triethoxysilane. Under the optimized conditions, a lamellar morphology of isobutyl-functionalized silicate sheets separated by layers of interdigitated surfactant molecules was obtained. Based on evidence from ^{29}Si MAS NMR, isobutyl groups remained covalently attached to silicon in the mesostructured product and the fraction of isobutyl-substituted silicon groups in the product was close to that fraction in the precursor mixture (ca. 10 mol %).

The TEM results show that clay particles in the PP-7K/iC$_4$-LMS blends had the highest lateral dimensions and the SWAXS data indicate that the iC$_4$-LMS particles were the most exfoliated in this comparison of clay materials. However, in contrast to the gelation observed in TMPD, composites obtained by melt blending iC$_4$-LMS with PP had only slightly higher G' values in the melt than neat PP. This modest effect on G′ might arise because the iC$_4$-LMS layers were not tough enough to endure the high shear stress resulting from the higher viscosity PP. Thus, the layers tended to break up, reducing their aspect ratios and the strength of the composites. In related work involving alkyl-functionalized lamellar silicates and aluminosilicates melt-blended with PS, it was observed that incorporation of aluminum, especially octahedral aluminum, within silicate layers enhanced the modulus of the PS-clay composite.[16,17] The aluminum was thought to enhance mechanical stability of clay sheets and reduce breakage of clay sheets by mechanical shear. In that system, PS-Cloisite® 20A nanocomposites exhibited the highest storage modulus, presumably because of mechanically stronger inorganic sheets. Further improvements in mechanical properties of blends with higher molecular weight PP might be achieved by embedding Al in the layers of iC$_4$-LMS, and we are currently working on preparing such mesophases.

We thank Dr. C. Fyfe (University of British Columbia) for access to his solid state NMR instrumentation, Dr. J. Shore (South Dakota State University) for obtaining ^{29}Si-MAS NMR spectra, Dr. L. Yao for ^{13}C and ^{1}H-NMR of PP, D. F. Eckel (GM R and D Center) for obtaining some of the TEM micrographs, L. Sauer (U of MN Characterization Facility) for assistance with SWAXS and M. Dolgovskij for GPC measurements.

References

1. Kato, M.; Usuki, A.; Okada, A. J Appl Polym Sci 1997, 63, 137.
2. Karger-Kocsis, J. Polypropylene: Structure, Blends, and Composites; Chapman and Hall: London, 1995.
3. Alexandre, M.; Dubois, P. Mater Sci Eng 2000, 28, 1.
4. Kato, M.; Usuki, A.; Okada, A. J Appl Polym Sci 1997, 66, 1781.
5. Cho, J. W.; Paul, D. R. Polymer 2001, 42, 1083.
6. Dennis, H. R.; Hunter, D. L.; Chang, D.; Kim, S.; White, J. L.; Cho, J. W.; Paul, D. R. Polymer 2001, 42, 9513.
7. Fornes, T. D.; Yoon, P. J.; Keskkula, H.; Paul, D. R. Polymer 2001, 42, 9929.
8. Kawasumi, M.; Hasegawa, N.; Kato, M.; Usuki, A.; Okada, A. Macromolecules 1997, 30, 6333.
9. LeBaron, P. C.; Wang, Z.; Pinnavaia, T. J. Appl Clay Sci 1999, 15, 11.
10. Okada, A.; Kawasumi, M.; Usuki, A.; Kojima, Y.; Kurauchi, T.; Kamigaito, O. Mater Res Soc Symp Proc 1990, 171, 45.
11. Ogawa, M.; Kuroda, K. Bull Chem Soc Jpn 1997, 70, 2593.
12. Wolf, D.; Fuchs, A.; Wagenknecht, U.; Kretzschmar, B.; Jehnichen, D.; Haussler, L.Eurofiller's 99; Lyon-Villeurbanne, 1999; p 6.
13. Nam, P. H.; Maiti, P.; Okamoto, M.; Kotaka, T.; Hasegawa, N.; Usuki, A. Polymer 2001, 42, 9633.
14. Carrado, K. A.; Xu, L.; Csencsits, R.; Muntean, J. V. Chem Mater 2001, 13, 3766.
15. Rausell-Colom, J. A.; Serratosa, J. M. Chemistry of Clays and Clay Minerals; Wiley-Interscience: New York, 1987.
16. Chastek, T. T.; Que, E. L.; Shore, J. S.; Lowy, R. J. I.; Macosko, C. W.; Stein, A. Polymer 2005, 46, 4421.
17. Chastek, T. T.; Stein, A.; Macosko, C. W. Polymer 2005, 46, 4431.
18. Southern Clay Products.http://www.nanoclay.com/(accessed January 4, 2007).
19. Fu, X.; Qutubuddin, S. Polymer 2001, 42, 807.
20. Garcia-Lopez, D.; Picazo, O.; Merino, J. C.; Pastor, J. M. Eur Polym J 2003, 39, 945.
21. Hancock, M.; Tremayne, P.; Carrick, B. Eur Plast News 1977, 4, 38.
22. Kurokawa, Y.; Yasuda, H.; Kashiwagi, M.; Oyo, A. J Mater Sci Lett 1997, 16, 1670.
23. Kurokawa, Y.; Yasuda, H.; Oya, A. J Mater Sci Lett 1996, 15, 1481.
24. Merinska, D.; Kovarova, L.; Kalendova, A.; Vaculik, J.; Weiss, Z.; Chmielova, M.; Malac, J.; Simonik, J. J Polym Eng 2003, 23, 241.
25. Oya, A.; Kurokawa, Y. J Mater Sci 2000, 35, 1045.
26. Pozsgay, A.; Frater, T.; Szazdi, L.; Muller, P.; Sajo, I.; Pukanszky, B. Eur Polym J 2003, 40, 27.
27. Zilg, C.; Dietsche, F.; Hoffmann, B.; Dietrich, C.; Mulhaupt, R. Macromol Symp 2001, 169, 65.
28. Beck, J. S.; Vartuli, J. C.; Roth, W. J.; Leonowicz, M. E.; Kresge, C. T.; Schmitt, K. D.; Chu, C. T.-W.; Olson, D. H.; Sheppard, E. W.; McCullen, S. B.; Higgins, J. B.; Schlenker, J. L. J Am Chem Soc 1992, 114, 10834.
29. Kresge, C. T.; Leonowicz, M. E.; Roth, W. J.; Vartuli, J. C.; Beck, J. S. Nature 1992, 359, 710.
30. Jaber, M.; Miehe-Brendle, J.; Le Dred, R. J Mater Sci 2004, 39, 1489.
31. Parikh, A. N.; Schivley, M. A.; Koo, E.; Seshadri, K.; Aurentz, D.; Mueller, K.; Allara, D. L. J Am Chem Soc 1997, 119, 3135.
32. Fujimoto, Y.; Shimojima, A.; Kuroda, K. Chem Mater 2003, 15, 4768.
33. Schmidt, D. F.; Qian, G.; Giannelis, E. P. Polym Mater Sci Eng 2000, 82, 215.
34. Shimojima, A.; Kuroda, K. Chem Lett 2000, 11, 1310.
35. Shimojima, A.; Kuroda, K. Langmuir 2002, 18, 1144.
36. Shimojima, A.; Sugahara, Y.; Kuroda, K. Bull Chem Soc Jpn 1997, 70, 2847.
37. Shimojima, A.; Sugahara, Y.; Kuroda, K. J Am Chem Soc 1998, 120, 4528.
38. Ogawa, M. Langmuir 1997, 13, 1853.
39. Herrera, N. N.; Letogge, J.-M.; Putaux, J.-L.; David, L.; Bourgeat-Lami, E. Langmuir 2004, 20, 1564.
40. Singh, A.; Haghighat, R. U.S. Pat. 6,057,035 (2000).

41. Scholte, T. G.; Meijerink, N. L. J.; Schoffeleers, H. M.; Brands, A. M. G. J Appl Polym Sci 1984, 29, 3763.
42. Dolgovskij, M. K.; Fasulo, P. D.; Lortie, F.; Macosko, C. W.; Ottaviani, R. A.; Rodgers, W. R. ANTEC 2003, 2255.
43. Burkett, S. L.; Sims, S. D.; Mann, S. Chem Commun 1997, 1769.
44. Sims, S. D.; Burkett, S. L.; Mann, S. Mater Res Soc Symp Proc 1996, 431, 77.
45. Goletto, V.; Dagry, V.; Babonneau, F. Mater Res Soc Symp Proc 1999, 576, 229.
46. Hall, S. R.; Fowler, C. E.; Lebeau, B.; Mann, S., Chem. Commun. 1999, 201.
47. Brinker, C. J.; Scherer, G. W. Sol-Gel Science: The Physics and Chemistry of Sol-Gel Processing; Academic Press: New York, 1990.
48. Christiansen, S. C.; Zhao, D.; Janicke, M. T.; Landry, C. C.; Stucky, G. D.; Chmelka, B. F. J Am Chem Soc 2001, 123, 4519.
49. Huo, Q.; Margolese, D. I.; Stucky, G. D. Chem Mater 1996, 8, 1147.
50. Stein, A.; Melde, B. J.; Schroden, R. C. Adv Mater 2000, 12, 1403.
51. Lin, C. J.; Hogan, T. E.; Hergenrother, W. L. Rubber Chem Technol 2004, 77, 90.
52. Brown, G.; Brindley, G. W. Crystal Structures of Clay Minerals and Their X-Ray Identification; Mineralogical Society: London, 1980.
53. Tolbert, S. H.; Landry, C.; Strucky, G. D.; Chmelka, B. F.; Norby, P.; Hanson, J. C.; Monnier, A. Chem Mater 2001, 13, 2247.
54. Loy, D. A.; Baugher, B. M.; Baugher, C. R.; Schneider, D. A.; Ramihian, K. Chem Mater 2000, 12, 3624.
55. Luckham, P. F.; Rossi, S. Adv Colloid Interface Sci 1999, 82, 43.
56. Moraru, V. N. Appl Clay Sci 2001, 19, 11.
57. Zhong, Y.; Wang, Q. J Rheol 2003, 47, 483.
58. Van Krevelen, D. W. Properties of Polymers: Their Correlation with Chemical Structures; Numerical Estimation and Prediction from Additive Group Contributions; Elsevier Science: Amsterdam, 1990.
59. Brandrup, J.; Immergut, E. H.; Grulke, E. A.; Bloch, D. R.; Abe, A. Polymer Handbook; Wiley: New York, 1999.
60. Marchant, D.; Jayaraman, K. Ind Eng Chem Res 2002, 45, 6402.